1 Introduction

The role of organic materials is essential in our daily life. In former times, the only possibility to achieve light was to ignite woods or oil, which are organic materials. Nowadays, organic semiconductors have gained extensive attraction due to their large-area and low-cost fabrication. Besides, the optoelectronic properties of organic semiconductors can be easily tuned by their convenient molecular design, which increases their potential to be applied in various kinds of electronics products.

Organic semiconductors are been an important material for numerous devices such as organic light-emitting diodes (OLEDs) [1–3], organic solar cells (OSCs) [4, 5], organic thin-film transistors [6, 7] and organic solid-state lasers (OSSLs) [8, 9]. Since there is high interest in the industry and technology field, a variety of organic semiconductors have been researched. Especially, OLEDs are been strongly promoted into commercial applications as the display of smartphones and televisions. OSSLs have the possibility to be another organic light emitter. Yet, it is still a young and challenging research topic. OSSLs provide another new horizon for simple, low-cost, time-saving, versatile, and environmentally-friendly fabrication of new and desirable laser structures. There is numerous literature about OSSLs. Diverse application fields have been found, such as lab-on-chip spectroscopy [10], absorption and transmission spectroscopy [11, 12], data/optical communication [13], refractive index sensor [14], vapour pressure detector [15] and etc.

The first-ever OSSL was discovered in 1967 when Rh6G doped in poly(methyl methacrylate) (PMMA) was found to be an organic gain medium [16]. Afterwards, much effort was done into this topic. One of the organic semiconductor lasers (OSLs) was reported, in which the materials were anthracene in doped and non-doped single crystals [17]. The first thin-film OLED was proposed by Tang and Van Slyke in 1987 [18]. This significant achievement of OLEDs contributes to a better understanding of the structural design and functions of organic materials. Subsequently, this leads to the significant development of OSLs. In 1996, Friend and Heeger introduced an OSL based on conjugated polymers by using poly(p-phenylenevinylene) (PPV) and PPV derivatives as gain medium [19, 20]. Later, Samuel's group introduced a polymer laser pumped by LED, in which a fluorene copolymer was used as the gain media [21]. In 2009, a deep-blue laser with a very low lasing threshold and high slope efficiency using monodisperse starburst macromolecular semiconductor as emitter was proposed [22]. A few years later, Gather et al. discovered the first observation of lasing behaviour in a living system with green fluorescent protein [23]. Recently, Adachi et al. demonstrated a quasi continuous-wave OSL based on near-infrared thermally activated delayed fluorescent emitters and the possibility of an electrically pumped organic laser [24–26]. Figure 1.1 shows the development milestones of organic gain media.

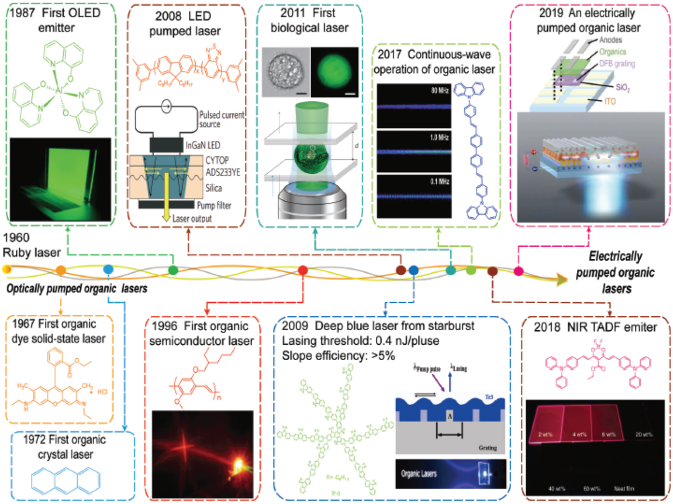

Figure 1.1: Timeline of development of organic main media.

To function as organic gain media, organic dyes have been dissolved in liquid solvents for the lasing purpose for decades [27]. However, this kind of operation can induce unnecessary evaporation of the solvents. To solve this problem, organic dyes can be doped in non-conjugated polymers, such as polystyrene (PS) and PMMA, which are suitable for OSSLs. This resulted laser is defined as organic dye lasers, which is quite similar to OSLs. According to Samuel el al., there are properties to make a division for organic semiconductors: (i) easy thin-film fabrication, (ii) high photoluminescence quantum yield (PLQY), and (iii) potential of charge transport [28]. There is abundant literature about organic dye lasers. It is observed that there are several sample designs for the dye-doped PS samples [14, 29–32]. On the other hand, the dye-doped PMMA samples were mostly based on only thin-film structure [33, 34].

In this work, the feasibility of organic dye-doped PMMA laser was studied. There were in total six different sample designs proposed to find out the sample model with the best performance. Next, the layer thickness of the gain medium and the resonator of the best sample model was manipulated to assure the outcome. Lasing properties like narrowing of Full Width at Half Maximum (FWHM) and lasing threshold were monitored. Besides, alternations of gain medium and resonator were performed to observe the effect on the lasing properties, in which the concentration of dye and the grating period were manipulated. Moreover, the workability of different organic dyes with PMMA was also determined. It was shown that organic dye-doped PMMA could function as a laser, which had an application potential.

2 General theory

In this chapter, one will get an overview of the general basics. At first, a short description of light propagation is elucidated here. Then, it is followed by a brief explanation of optical waveguides, which are an example of the medium for light propagation. Besides, general information about organic semiconductors is shown, as the material used in this research is mainly made up of organic material. Moreover, two important characteristics of organic materials are briefly described, which are the photoluminescence quantum yield and the fluorescence lifetime. Furthermore, a compact description of quenching is presented to understand the processes, which can reduce the intensity of fluorescence.

Every single section provides elementary theories, which provide adequate physics information for the readers to understand this work better. Detailed explanations can be found on the indicated references.

2.1 Light Propagation

Electromagnetic radiation can be defined as a form of energy. In this form of energy, all the waves of the electromagnetic field such as gamma rays, X-rays, ultraviolet radiation, visible light, infrared, radio waves, etc are included. According to Figure 2.1, visible light is only a very small portion of the total electromagnetic radiation. Based on the DIN 5031-7, visible light starts from 380 nm to 780 nm [35]. Radiation energy can be induced by the propagation of electromagnetic radiation, which can be calculated using the equation below:

$$E_{\text{radia}} = h\upsilon = \frac{hc}{\lambda} = \frac{hc}{2\pi}k \tag{2.1}$$

whereas E_{radia} is the radiation energy, h is the Planck constant, υ is the frequency, c is the velocity of light in a vacuum, λ is the wavelength and k is the wavenumber.

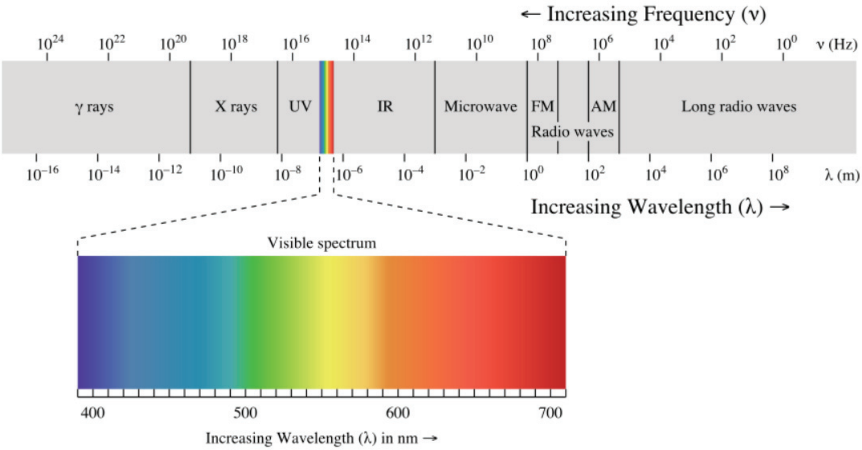

Figure 2.1: Electromagnetic spectrum with labelled regions. Reprinted from [36].

The concept of light propagation is proposed that the movement of the energy of the electromagnetic waves can be achieved from one point to another. Electromagnetic waves contain electric and magnetic components. Meanwhile, the light propagation is not the same as mechanical waves because no material is required for their energy transportation. Therefore, light is capable to pass through the vacuum of outer space with a velocity $c = 3 \times 10^8\,\mathrm{m\,s^{-1}}$ [37, 38]. The wavelength of the frequency of the light is in a relationship with the light velocity, which is shown in the following equation:

$$\upsilon = \frac{c}{\lambda}. \tag{2.2}$$

When there is light propagation in a medium, the velocity of light becomes less than the velocity in a vacuum. The actual velocity of light relies on the optical density of the material. This is because optical density is determined as the degree to which a medium can refract the transmitted light. In short, the whole mechanism is illustrated by the refractive index n_r. When the refractive index rises, the velocity of light in the medium decreases. n_r of vacuum is determined as 1, which is used as a reference. For instance, n_r of water is 1.33, which means the light propagation in water is 1.33 times slower compared to vacuum. n_r can be calculated using

$$n_r = \frac{c}{\nu} \tag{2.3}$$

whereas ν is the phase velocity of light in the material.

Figure 2.2 presents an overview of the mechanisms when there is an interaction of light with another medium with a different refractive index. Absorption exists when the light is taken in, which is usually converted into heat if it is not reemitted as luminescence. Besides, another mechanism is called transmission when the electromagnetic waves are able to pass through the medium. After transmission, the angle of the light can be different compared to incident light as it is refracted. The angle of refraction is based on the Snell's law ($n_1 \sin(\theta_i) = n_2 \sin(\theta_{rr})$). On top of that, reflection takes place, when the light rebounds at the interface between two media with different refractive indices. Based on the law of reflection, the light is reflected with the same angle to the surface normal as the incident ray under the assumption that the surface of the interface is mirror-like ($\theta_i = \theta_{rl}$), otherwise, scattering may occur if the surface is too rough.

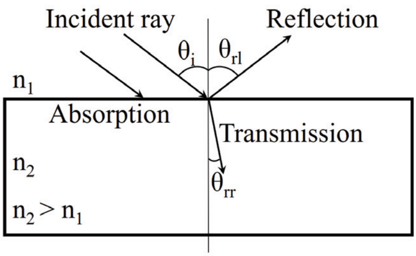

Figure 2.2: When light reaches an object with different refractive indices, reflection, absorption and transmission will take place.

2.2 Optical Waveguide

By using an optical waveguide, it is understood to be the guidance of an electromagnetic wave in a suitable structure. The light undergoes a prescribed direction so that it can be guided to reach desired optoelectronic achievements. There are different types of optical waveguides. Here, the planar waveguide and the striped waveguide are concisely presented.

2.2.1 Planar Waveguide

The guidance of an electromagnetic wave in a planar thin-film is based on the principle of total reflection. A planar waveguide consists of optical layers with different refractive indices. The layer, which guides the light, has a refractive index of n_f. It is surrounded by a bottom layer (which is normally a substrate) with a refractive index of n_s and an upper layer (in the simplest case air) with a refractive index of n_c. If $n_s = n_c$, the waveguide is symmetrical, otherwise, it is an asymmetrical planar waveguide.

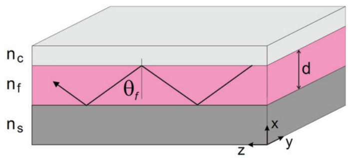

Figure 2.3: Structure of a planar waveguide. Reprinted from [39].

Figure 2.3 shows an example of a stack of layers, which is under the idealized assumption of infinite extension in the y- and z-directions. Transmission of an electromagnetic wave in the guiding layer would be possible if the refractive indices of the layers satisfy the inequality of $n_c \leq n_s \leq n_f$. Light performs a zigzag movement in the z-direction at an angle between the boundary layers. For the critical angle of total reflection in the guiding layer, $\theta_f > \theta_s, \theta_c$, in which θ_s and θ_c are in the relationship with the refractive index of the respective material like the equations below:

$$sin\theta_c = \frac{n_f}{n_c} \ and \ sin\theta_s = \frac{n_f}{n_s}. \tag{2.4}$$

The propagated waves can be distinguished into transverse electrical (TE) and transverse magnetic (TM). In TE waves, the electric field vector is perpendicular to the plane of incidence (x-z direction), whereas the magnetic field vector of TM waves is perpendicular to the direction of propagation. In addition to the condition of total reflection, every guided wave must "fit into" the guiding layer. In the x-direction, the wave components must interfere perpendicularly to the interfaces, to interfere with the standing waves. For this, the reflection must be in phase with x-components of the electromagnetic waves to provoke constructive interference. When these conditions are fulfilled, it is called a glancing angle, which ensures the propagation of discrete waves. This is defined as mode. A wave, which propagates in the z-direction, is described by the phase constant of the propagation coefficient β:

$$\beta = kn_f sin\theta \tag{2.5}$$

whereas k is the wave vector, which can be determined according to:

$$k = \frac{2\pi}{\lambda} = \frac{\omega}{c} \tag{2.6}$$

whereas ω is the angular frequency. For those under the angle of total reflection, the incident waves together with the reflected waves will have an effective refractive index n_{eff} as follow:

$$n_{eff} = n_f sin\theta = \frac{\beta}{k}. \tag{2.7}$$

The effective refractive index is a mode-specific variable, which is determined by all refractive indices. Thus, it depends on all the layers involved in the thin-film. A different effective refractive index applies to each propagation of mode. The relation $n_c \leq n_s \leq n_{eff} \leq n_f$ is generally valid. The following applies to the condition of the in-phase superposition:

$$kdn_f cos\theta_m - \Phi_c - \Phi_s = m\pi \tag{2.8}$$

whereas d is the thickness of the layer, m is the order of the mode and θ_m is the associated propagation angle, Φ_c and Φ_s are the phase shift at the respective interfaces according to the Goos-Hänchen effect [40, 41]. In contrast to the observation of electromagnetic waves as optical rays, the standing waves are not completely reflected at the interfaces. Part of the field intensity penetrates the adjacent layer and drops exponentially. This field portion is named as evanescent field [42]. The angle of the phase difference at the interfaces is calculated differently for TE and TM modes:

$$tan\Phi_{c,s}(TE) = \frac{\sqrt{n_f^2 sin^2\theta - n_{c,s}^2}}{n_f cos\theta} \tag{2.9}$$

$$tan\Phi_{c,s}(TE) = \frac{n_f^2}{n_{c,s}^2}\frac{\sqrt{n_f^2 sin^2\theta - n_{c,s}^2}}{n_f cos\theta} \tag{2.10}$$

d from Equation 2.8 plays an important factor in the existence of the guided light waves in the thin-film. For a certain layer thickness, only a limited number of modes can propagate. The first mode is also called the fundamental mode, which requires a certain minimum thickness ($d_{cut-off}$). In general, the minimum thickness (d_m) for the possible order of TE modes is calculated by using [43]:

$$d_m = \frac{\lambda}{2\pi}(n_f^2 - n_s^2)^{-\frac{1}{2}}(arctan\sqrt{\frac{n_s^2 - n_c^2}{n_f^2 - n_s^2}} + m\pi) \tag{2.11}$$

In Figure 2.4, the minimum thickness of the guiding layer for the fundamental mode TE_0 and the first subsequent TE_1 mode is shown, which is calculated according to Equation 2.11. It is an asymmetrical waveguide, as the refractive indices of the bottom layer (n_s of silicon dioxide = 1.46) and the upper layer (n_c of air = 1) are not the same. It is calculated for the spectral range from 550 nm to 650 nm based on the needs in this research. When the only fundamental mode is capable of propagation (single-mode), the layer thickness must be at least d_0. If the layer thickness exceeds the value d_1, TE_1 mode will be able to propagate [43].

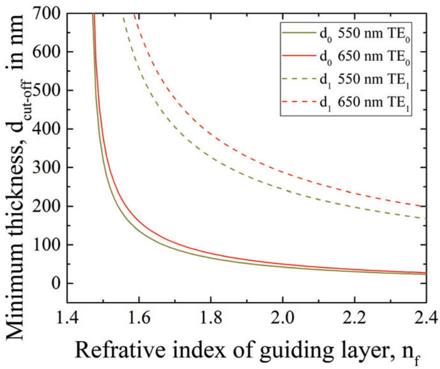

Figure 2.4: Minimum layer thickness $d_{cut-off}$ for TE_0 and TE_1 modes based on Equation 2.11.

In order to determine the field distribution of E(x) and H(x), the Helmholtz equations need to be solved. A simulation program based on Mathematica® was applied for the calculations in this work, which was developed by Rabe et. al. in his dissertation [44]. The fill factor (Γ_j), in which the wave intensity in a layer was distributed, can be calculated by using:

$$\Gamma_j = \frac{\int_{x_{j-1}}^{x_j} \left|E^2\right| dx}{\int_{-\infty}^{\infty} \left|E^2\right| dx}. \tag{2.12}$$

2.2.2 Stripe Waveguide

Stripe waveguide is different from the planar waveguide, as it has an additional lateral waveguide, which can be produced by having a rectangular structure in the yz-plane. The guiding waveguide is generally named core, while the surrounding material is called cladding. This structure has an impact on the effective refractive index and the propagation of modes in the waveguide, eventually.

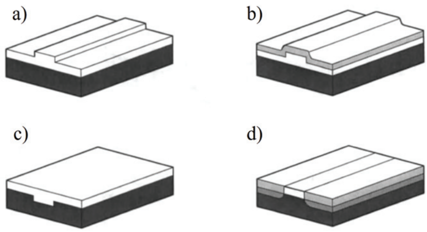

Figure 2.5: Different forms of stripe waveguide are illustrated: (a) ridge, (b) inverted ridge, (c) buried and (d) diffused. Reprinted from [45].

In Figure 2.5, there are some options for realising a stripe waveguide. The ridge waveguide can be produced when the thickness of the guiding material in the middle area of the stripe waveguide is increased (see Figure 2.5(a)). As in Figure 2.5 (b), when the ridge waveguide corresponds in the direction of the substrate or cladding, an inverted ridge waveguide is presented. If the stripe waveguide is sheathed from above as Figure 2.5 (c) and (d), it is referred to as a buried or diffused waveguide. In such a way, single-mode operations can take place with a relatively larger height and width. An advantage can be found in a diffusion waveguide. As the field distribution in the core can be cylinder-symmetrical, a high coupling efficiency is possible in single-mode operations with suitable adaptation. [45, 46].